

A SIMIND Monte Carlo Simulation Study on CdTe and NaI (TI) Thickness as Detectors of a Small Animal SPECT System

Samira Abbaspour ¹, Babak Mahmoudian ², Seyed Rasoul Zakavi ³, Jalil Pirayesh Islamian ^{4*} 

¹ Department of Medical Physics, School of Medicine, Tehran University of Medical Sciences, Tehran, Iran

² Department of Nuclear Medicine, Faculty of Medicine, Tabriz University of Medical Sciences, Tabriz, Iran

³ Nuclear Medicine Research Center, Mashhad University of Medical Sciences, Mashhad, Iran

⁴ Department of Medical Physics, Faculty of Medicine, Tabriz University of Medical Sciences, Tabriz, Iran

*Corresponding Author: Jalil Pirayesh Islamian
Email: pirayeshj@gmail.com

Received: 11 August 2021 / Accepted: 25 December 2021

Abstract

Purpose: Micro Single Photon Emission Computed Tomography (Micro-SPECT) system has recently been introduced on nuclear medicine in the preclinical and research in which NaI (TI) and Cadmium Telluride (CdTe) are used as the gamma-ray detectors with more generally use of NaI (TI). The present study aimed to evaluate different thicknesses of the NaI (TI) and (CdTe) detectors on functional parameters of a micro-SPECT system.

Materials and Methods: A Micro-SPECT system with CdTe semiconductor detector and a hexagonal parallel hole collimator with a hole diameter of 0.11 mm, high of 24.05 mm, and septal thickness of 0.016 mm was simulated by Simulating Medical Imaging Nuclear Detectors (SIMIND) Monte Carlo program. The system performance was assessed by comparing the functional parameters, including system efficiency, sensitivity, energy and spatial resolution with the NaI (TI) detector. The simulated scans of a ^{99m}Tc point source, a digital micro-Jacszack phantom, and a voxelized MOBY mouse phantom with the system were prepared to evaluate image quality.

Results: The functional parameters; sensitivity, efficiency, planar spatial resolution, and image contrast of CdTe detector were determined 1.4, 1.2, 1.7, and 1.8 times higher than those of NaI (TI), respectively. Moreover, the calculated energy resolution of CdTe and NaI (TI) detectors was obtained 6.2% and 10.2% at 141 KeV, respectively. In the filtered back projection (FBP) reconstructed images of the micro-Jacszack phantom, minimum detectable size of the cold rods with CdTe and NaI (TI) detectors were obtained 0.79 mm and 0.95 mm, respectively.

Conclusion: The imaging system with a 5.5 mm thickness CdTe detector provided better image quality and showed considerable efficiency.

Keywords: Cadmium Telluride; Resolution; Image Quality; Micro Single Photon Emission Computed Tomography; Simulating Medical Imaging Nuclear Detectors Monte Carlo.

1. Introduction

The small animal Micro Single Photon Emission Computed Tomography (Micro-SPECT) system was considered a powerful instrument in biological studies and provides useful information about physiological, functional, and pathological data in molecular imaging [1, 2]. The detector plays a key role in the quality of the images and is responsible for absorbing and detecting the high-energy photons as the main compartment of the photon interaction [3, 4]. High spatial resolution, high energy resolution, better sensitivity, and high quantum detection efficiency are the main factors in Micro-SPECT imaging systems that are affected by the material and geometry of the detector [5, 6]. Therefore, providing a good efficiency for a Micro-SPECT system is based on the improvement of the detector [1, 4].

Sodium Iodide activated by Thallium [NaI (Tl)] scintillation detector, as a conventional detector, induces high luminous efficiency and is costly effective [4, 7]. Generally, the limitations are related to its low intrinsic sensitivity, low energy and spatial resolution, and hygroscopic feature [4]. Low density (3.76 g/cm^3) of the detector material with a long radiation length contributes to the related lower spatial resolution [4]. In order to overcome these limitations, Cadmium Telluride (CdTe) and Cadmium Zinc Telluride (CdZnTe) detectors, as favorable semiconductor materials and main alternatives for the scintillation detectors, have been introduced [8]. The CdTe detector has generally some priorities over NaI (Tl) detector considering energy resolution, sensitivity, and detection efficiency; also it leads to an ultra-high spatial resolution SPECT system [9]. The CdTe semiconductor detector has a high atomic number (Cd: 48 and Te: 52) with a high density (5.85 g/cm^3), which provides a better absorption characteristic with high detection efficiency and better spatial resolution [10-13]. Furthermore, as a pixelated detector, its intrinsic spatial resolution is equal to the pixel size [14].

Semiconductor detector eliminates the need for bulky Photomultiplier Tubes (PMTs) with an improved energy resolution, also provides a thin and lightweight camera head and gives the flexibility to design the camera [15-17]. Moreover, the detector has a wide band gap (1.44 eV) which offers its operation at room temperature. Notably, the semiconductors have a lower carrier creation energy and low scatter count in comparison with the scintillators [18].

Monte Carlo simulations were successfully used in modeling the gamma camera and collimator design [19, 20]. The Monte Carlo simulation is an appropriate tool in the field of nuclear medicine and is also an effective tool when experimental evaluations are not practical or experiments are excessively expensive [21]. Besides, digitized phantoms, as the emission sources for quantitative calculations, have facilitated molecular imaging research and the improvement of new imaging equipment [20].

In this study, Simulating Medical Imaging Nuclear Detectors (SIMIND) Monte Carlo program was used to simulate a Micro-SPECT system with CdTe and NaI (Tl) detectors as well as an ultra-high resolution parallel-hole collimator. Notably, several main functional parameters, including system efficiency, sensitivity, energy and spatial resolution, and image quality were determined and compared between the two investigated detectors at different thicknesses from the output files. Although several studies investigated and compared the parameters of the two above-mentioned detectors based on the different isotopes, various source to collimator distances and collimator lengths [22, 23], to the best of our knowledge, there is no study determining the appropriate thickness of CdTe detector with regarded to NaI (Tl) detector using SIMIND Monte Carlo program in a Micro-SPECT system.

2. Materials and Methods

2.1. Simulation Set-Up

A Micro-SPECT system consisting of two different detector materials, including a CdTe semiconductor and a NaI (Tl) scintillator detector with a similar collimator geometry were simulated by SIMIND Monte Carlo simulation program version 6.0, developed by Professor Michael Ljungberg, Sweden [24]. The output files of the program, including *.smc, *.bis, *.prn, *.bim, *.h00, *.a00, *.hct, and *.ict were used for simulation, extracting functional, and imaging parameters.

The accuracy and usefulness of the code had previously been confirmed [25-28]. The CdTe semiconductor detector was considered with a pixel size of $0.5 \times 0.5 \text{ mm}^2$ and an active area of $45.7 \times 45.7 \text{ mm}^2$. The intrinsic spatial resolution of the detector was considered 0.5 mm Full Width at Half Maximum (FWHM), equal to the pixel size [29]. The corresponding values for the NaI (Tl) scintillator detector that assembled to the position-sensitive photomultiplier tubes, were considered 1×1

mm² and 45.7 × 45.7 mm², respectively [20]. The intrinsic spatial resolution of the detector was considered 3.8 mm FWHM (in thickness of 0.95 cm) [29, 30]. The different thicknesses of the detectors, ranged from 1 to 9.5 mm, with the steps of 0.5 mm was simulated for the study.

2.2. Assessment of System Performance

2.2.1. Functional Parameters

To assess the system functional parameters, a ^{99m}Tc point source with an activity of 3.7 MBq (with a 1.1 mm inner diameter) was centrally located along the Useful Field Of View (UFOV). A symmetrical energy window width was set to 15% on the ^{99m}Tc photopeak spectrum. The point source was emitted by gamma-rays in the direction of a 4π steradian at 2.5 cm away from the detector surface equipped with an ultra-high resolution collimator [31]. The pixel size of the simulated planar point source images was considered 0.035 cm and saved in a matrix of 128×128 pixels. The measurements of the efficiency, sensitivity, energy spectra, energy resolution, and planar spatial resolution of the CdTe and NaI (Tl) detectors were calculated according to the National Electrical Manufacturers Association (NEMA) Standard [32, 33]. The spatial resolution was calculated as a function of FWHM from the plotted profiles of the Point Spread Function (PSF).

Also, both of cameras were equipped with an ultra-high resolution parallel-hole collimator which was composed of a lead plate with hexagonal holes in the diameters of 0.11 mm, the septal thickness of 0.016 mm, and a height of 24.05 mm. Also, a voxelized MOBY mouse phantom and a computational micro- Jaszack Deluxe phantom (model ECT/DLX/P) were used for the study. The SPECT simulation set-up with a MOBY mouse simulated phantom is provided in Figure 1.

The sensitivity was measured with the area under the PSF or in terms of counts per second per MBq. An energy pulse height distribution was acquired for 10 million counts/projection, also the energy resolution was calculated from FWHM of the ^{99m}Tc photopeak [14, 34].

2.3. Image Analysis (Reconstructed Spatial Resolution, Image Contrast and Signal to Noise Ratio)

To evaluate the SPECT reconstructed spatial resolution and image contrast, a computational micro- Jaszack

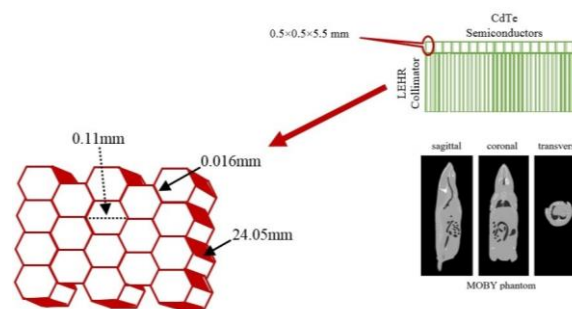


Figure 1. The SPECT simulation set-up with a Moby mouse simulated phantom

Deluxe phantom (model ECT/DLX/P) was used (Figure 2) [28]. The phantom, filled with 370 MBq of ^{99m}Tc solution, was simulated at a distance of 2.5 cm from the detector. The scan parameters were included matrices of 128 × 128 pixels, 128 views, 360° clockwise gantry rotation, zoom factor of 1 with a pixel size of 0.035 cm and 10 million events per projection. The reconstructed spatial resolution was determined by the smallest detectable sector of cold rods in the phantom. Also, the image contrast was determined in Regions Of Interest (ROI) occupied by the six cold spheres and also the background of the phantom according to the following Equation 1 [35]:

$$\% \text{Contrast of cold spheres} = \left(1 - \frac{M_{smin}}{M_{bmax}}\right) \times 100 \quad (1)$$

Where M_{smin} and M_{bmax} are the minimum and maximum count/pixel values in the ROIs for the cold spheres and background, respectively. Similar ROIs and slices were utilized to process all the reconstructed images of the phantom.

In order to calculate the Signal to Noise Ratio (SNR) of the images, as the ratio of mean value to Standard Deviation (SD) in the Volume Of Interest (VOI) [36], the Amide software (version 1.0.4) was used to draw three

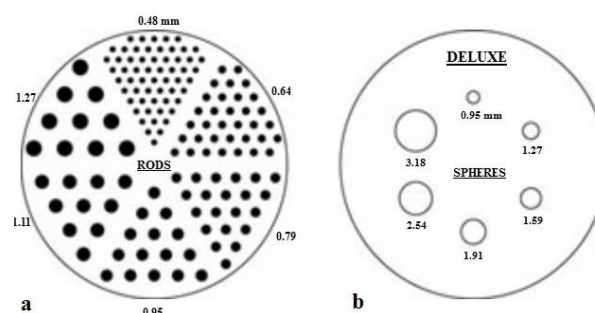


Figure 2. (a) A cross-sectional schematic drawing of a Deluxe micro-Jaszack Plexiglas phantom showing 148 rods in 6 sectors (0.48, 0.64, 0.79, 0.95, 1.11, and 1.27 mm), and (b) 6 spheres, (0.95, 1.27, 1.91, 1.59, 2.54, and 3.18 mm)

1-cm spheres onto the uniformity section of micro-Jaszack phantom (Figure 2).

The projection data of the micro-Jaszack phantom were reconstructed using local prepared the Filtered Back Projection (FBP) algorithm with a Ramp filter and then a post filter of Butterworth with a cutoff frequency of 0.25 cycles/cm and an order of 5. Since the projections of the SIMIND-simulated SPECT are without noise, Poisson noise was added proportionally to the ordered dose.

Also, a voxelized MOBY mouse phantom consisting of 202 slices with a pixel width of 0.045 cm and array size of 256×256 was used for simulating the clinical situation on the liver lesion detectability [6, 20]. We considered the liver of the MOBY as a target organ and inserted a cold (-125 Bq/voxel) and a hot lesion (125 Bq/voxel), both with a diameter of 2 mm in the right lobe of the liver. The scan parameters and reconstruction methods were the same as performed for the micro-Jaszack phantom. The detectability of the lesions, on the reconstructed images prepared from SPECT scanning of the phantom with different thicknesses of the detectors, were analyzed by visual inspection. Then, the contrast of the cold lesion was quantitatively calculated based on the previous formula (Equation 1) and for hot lesion was calculated using Equation 2:

$$\%Contrast = \frac{|M_s - M_b|}{|M_s + M_b|} \times 100 \quad (2)$$

Where, M_s is stated as the mean activity values in the ROIs occupied by the hot lesions, and M_b is the mean activity values of liver background [26].

Also, the calculation of SNR was the same as performed for the micro-Jaszack phantom, except the VOIs were chosen in the liver of MOBY phantom.

3. Results

3.1. Functional Parameters of the CdTe and NaI (TI) Scanners

Figures 3a and 3b show the results on the efficiency and sensitivity of both of the systems as a function of the CdTe and NaI (TI) detector thickness for a ^{99m}Tc point source scanning with the SIMIND simulated micro-SPECT system. The mean value of the efficiency was obtained 0.817 and 0.701, for those detectors (Figure 3a). Additionally, the mean value of the sensitivity for the investigated thicknesses was obtained 0.679 and 0.497 cps/MBq, respectively, for CdTe and NaI (TI) detectors (Figure 3b). As seen from the figures, there is a linear relationship between the efficiency and sensitivity of the detectors and their thicknesses. Meanwhile, the system with a CdTe detector provided about 1.2 and 1.4 times better efficiency and sensitivity in comparison with the NaI (TI) detector, respectively.

Figure 3c depicts FWHMs from the PSF for ^{99m}Tc point source scanning with CdTe and NaI (TI) scanners at 2.5 cm away from the detector surface. As expected, the spatial resolution decreased with increasing the detector thickness. The value for NaI (TI) detector was obtained about 1.7 times greater than CdTe detector. FWHM for 5.5 mm for the CdTe and NaI (TI) scanners were calculated as 0.69 and 1.2 mm, respectively (Figure 4a).

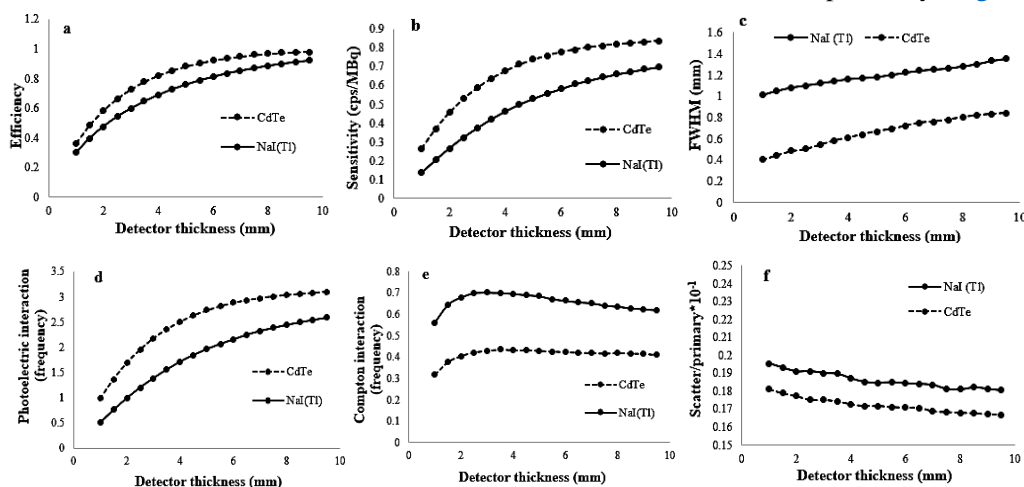


Figure 3. Scatter curves of the effect of CdTe and NaI (TI) detectors with different thicknesses (ranged from 1 to 9.5 mm) on functional parameters, including (a) efficiency, (b) sensitivity, (c) FWHM, (d) photoelectric interaction, (e) Compton interaction and (f) Scatter to a primary ratio of a ^{99m}Tc point source was scanned at 2.5 cm away from the detector surface with a 15% energy window width

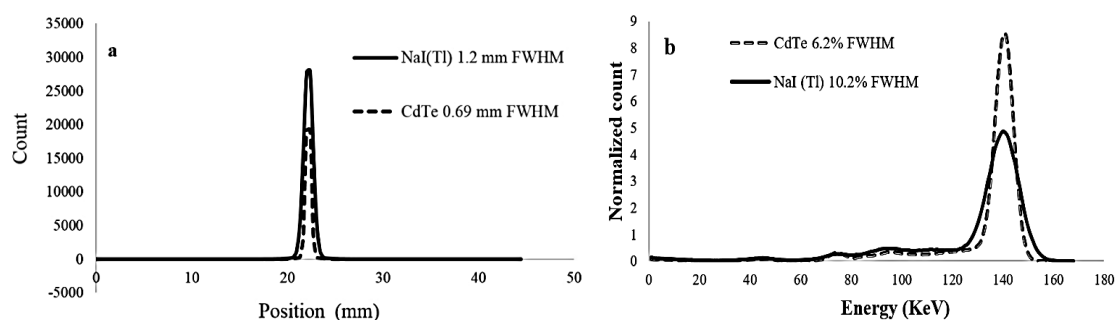


Figure 4. (a) The point spread function fitted of a ^{99m}Tc point source planar scanning at 2.5 cm away from the detector surface with a 15% energy window width for CdTe, and NaI (Tl) detectors, and the resulted energy spectra (b)

The results in photoelectric and Compton interactions for the thicknesses of CdTe detector compared to the NaI (Tl) detector for a ^{99m}Tc point source scanning in the selected window width (Figures 3d and 3e) showed that increasing detector thickness either increased the photoelectric and Compton interactions. The photoelectric interaction and also the Compton interaction fraction for the 5.5 mm CdTe and NaI (Tl) detectors were calculated as 2.813, 2.062, 0.4264, and 0.6701, respectively.

The simulated energy spectra for the point source located at a 2.5 cm distance from the detector surface with the 15% photopeak window width are shown in Figure 4b.

3.2. Image and Quantitative Data of the Jaszczak Phantom SPECT

Figure 5 shows the reconstructed images of cold rods and spheres of the micro-Jaszczak phantom. According to this Figure 5a and c, the smallest visible rods were detected at 0.79 mm and 0.95 mm diameters, respectively, for CdTe and NaI (Tl) detectors. The calculated contrast in the reconstructed SPECT images of simulated 0.95, 1.27, 1.59, 1.91, 2.54, and 3.18 mm cold spheres of Jaszczak phantom with CdTe and NaI (Tl) detectors were found 31.09%, 44.17%, 73.8%, 82.57%, 84.97%, 88.15% and 26.63%, 34.7%, 60.36%, 63.07%, 81.74%, 84.22%, respectively (Figures 5b and 5d). Also, the average SNR of CdTe and NaI (Tl) detectors was achieved at 23.14 and 17.68, respectively.

3.3. Image and Quantitative Data of the MOBY SPECT Imaging

Figures 6a and 6b illustrate the reconstructed MOBY liver SPECT transaxial images prepared by CdTe and NaI (Tl) detectors. Visual assessing of the qualities of the image showed that the detectability and sharpness of cold

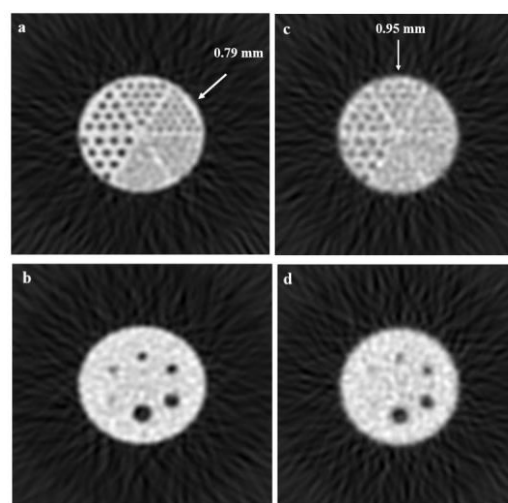


Figure 5. The FBP reconstructed images of the micro-Jaszczak phantom when scanned with a micro-SPECT system equipped with a 5.5 mm CdTe detector: cold rods (a), cold spheres (b), and the similar scans with a 5.5 mm NaI (Tl) detector: cold rods(c), and cold spheres (d)

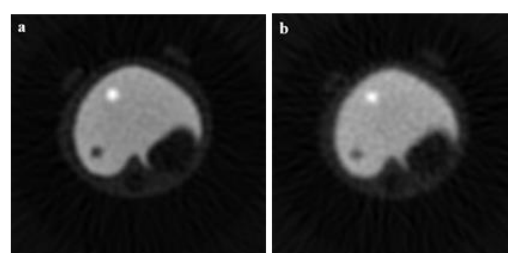


Figure 6. The FBP reconstructed images of the MOBY mouse phantom: transverse view of the 2 mm cold and hot lesions in the right lobe of the liver of the MOBY prepared with a 5.5 mm CdTe detector (a) and NaI (Tl) detector (b)

and hot lesions in the liver with the CdTe were better than the NaI (Tl) detector. The contrast of hot and cold lesions with the detectors was determined at 26% and 53.6% for the CdTe and 21% and 36.3% for NaI (Tl) scanners, respectively. Furthermore, the average SNR in the liver for the images reconstructed of MOBY phantom was obtained at 47.47 and 39.02 for CdTe and NaI (Tl) detectors,

respectively. The calculated energy resolution was obtained 6.2% and 10.2% for the CdTe and NaI (Tl) detectors, respectively.

4. Discussion

Performance of a micro-SPECT imaging system equipped with CdTe and/or NaI (Tl) detectors was evaluated by simulated scanning of a ^{99m}Tc point source, a digital Jaszack phantom, and a voxelized MOBY mouse phantom with the SIMIND Monte Carlo program.

In general, the high intrinsic sensitivity of the CdTe scanner causes a reduction in statistical noise [14]. According to our results, for occurring the 90% efficiency at 141 KeV, 5.5 mm and 9.5 mm thicknesses were needed for CdTe and NaI (Tl) detectors, in that order. In addition, in the 5.5 mm thickness of the CdTe and NaI (Tl) detectors, the sensitivity was obtained 0.7602 cps/MBq and 0.5574 cps/MBq, respectively. Notably, for obtaining the 0.7602 cps/MBq sensitivity by NaI (Tl) detector, 9.5 mm thickness was needed, which was a considerably higher thickness for obtaining the same sensitivity by CdTe detector. In a study by Ryu *et al.* on the 1mm CdTe detector, they have shown an efficiency of 24.5% and sensitivity of 0.354 cps/kBq by using a ^{99m}Tc point source of 1 MBq [37]. They have expressed that, the efficiency can be increased by using a thicker CdTe detector, which brings a better sensitivity for high resolution and contrast. However, it seems that the results of Ryu *et al.* and the current study are different in which the different source activities can be the main factor.

Studies on proper thickness for the CdTe semiconductor have suggested a thickness of 5 mm or more to obtain a stopping power of at least 75% [14, 38]. In a study on the imaging performance of two compact gamma detector prototypes: a CdTe semiconductor and a LaBr₃ scintillator detector, it was demonstrated that the intrinsic efficiency of detector was obtained 83% for 5 mm thickness of scintillator compared to 45% for 1 mm of the semiconductor at 122 KeV [39]. In this regard, measurements on the Si (Li) semiconductor detector showed that a 6 mm thickness of detector is needed for achieving 90% efficiency with an energy resolution of 8.5% FWHM for the emissions of ^{125}I [40].

The higher photoelectric to Compton scattering ratio has an effect on better detection efficiency, and so a high stopping power of the CdTe semiconductor detector may be related to the high atomic number and higher density

of the detector, respectively. Further, the high photoelectric fraction makes it possible to construct a thinner detector [in comparison with NaI (Tl)] and subsequently improves the spatial resolution [22].

Therefore, the CdTe detector provides improved spatial resolution as compared to the NaI (Tl) detector. The intrinsic spatial resolution of the CdTe detector was considered 0.5 mm, the same as the pixel size, and related to the unique collection of the created electrons and holes by the exposed photons, collected by a small electrode for each pixel. Furthermore, the detector can distinguish small structures, and therefore it is suitable for biomedical research and molecular imaging [29, 41].

The CdTe semiconductor detector decreased the scatter count compared to the NaI (Tl) by direct conversion of gamma-ray photons to the electrical signal [42]. Our study showed that the frequency of scattering photons with NaI (Tl) detector was about 1.3 times higher than the CdTe detector. The higher the scatter rejection of the CdTe detector, the better the energy resolution [15].

According to Figure 4b, the energy spectra of the CdTe is sharper and higher in photopeak than the NaI (Tl), due to decreasing scatter counts and increasing count rate which provided better contrast and resolution in the images. On the other hand, the calculated energy resolution for the CdTe and NaI (Tl) detectors (6.2% and 10.2% FWHM), agreed with the theoretical values (6% and 9.9%) respectively [29, 30]. The superior energy resolution of the CdTe detector allows better separation of two energy peaks for ^{99m}Tc than were possible with the NaI (Tl) detector and so useful for dual-isotope studies and improves SPECT measurements [43, 44]. Besides, the narrower energy window could be produced by decreasing the number of photons that have undergone Compton scattering [4].

It must be mentioned that Qi *et al.* reported the smallest visible cold rods with NaI (Tl) detector, to 1.6 mm [34], and in our study also the measure obtained 0.95 mm (Figures 5c). This variation may come from employing different collimator types, i.e. the ultra-high resolution parallel-hole collimator compared to their pinhole. Also, according to Figures 5b and 5d, the CdTe detector provides an improved image contrast, 12%, than the NaI (Tl) detector for the detector thickness of 5.5 mm. As a whole, in order to have an absolute suggestion, it may need to extend the study using a multi-pinhole collimator and compare the results.

All in all, from the point of view of image quality, higher SNR by CdTe, results in high-quality images. In addition,

the CdTe detector with a thickness of 5.5 mm provided a high-quantum efficiency and a high-energy resolution that make the semiconductor an appropriate candidate for the detection of photons at the effective energy of the ^{99m}Tc for small animal imaging.

5. Conclusion

The simulated micro-SPECT system with a 5.5 mm CdTe detector provides a considerable improvement on the system performance, sensitivity, spatial and energy resolution, and image quality.

Acknowledgments

This work was financially supported by the office of the vice president for research in Tabriz University of Medical Sciences, Tabriz, Iran (Grant # 8971). The authors wish to thank Prof. Michael Ljungberg at the department of medical radiation sciences, Lund University, Lund, Sweden, for his sincere consult on the SIMIND simulation of the present study.

References

- Alireza Sadremomtaz and Zeinab Telikani, "Validation and optimization studies of small animal SPECT using GATE Monte Carlo simulation." *Nuclear Instruments and Methods in Physics Research Section A: Accelerators, Spectrometers, Detectors and Associated Equipment*, Vol. 915pp. 94-101, (2019).
- Robert S Miyaoka and Adrienne L Lehnert, "Small animal PET: a review of what we have done and where we are going." *Physics in Medicine & Biology*, Vol. 65 (No. 24), p. 24TR04, (2020).
- Thomas A Holly et al., "Single photon-emission computed tomography." *Journal of nuclear cardiology*, Vol. 17 (No. 5), pp. 941-73, (2010).
- Todd E Peterson and Lars R Furenlid, "SPECT detectors: the Anger Camera and beyond." *Physics in medicine and biology*, Vol. 56 (No. 17), p. R145, (2011).
- Jorge Mejia et al., "Performance assessment of the single photon emission microscope: high spatial resolution SPECT imaging of small animal organs." *Brazilian Journal of Medical and Biological Research*, Vol. 46 (No. 11), pp. 936-42, (2013).
- Roel Van Holen, Bert Vandeghinste, Karel Deprez, and Stefaan Vandenberghe, "Design and performance of a compact and stationary microSPECT system." *Medical physics*, Vol. 40 (No. 11), p. 112501, (2013).
- Young-Jin Lee, Dae-Hong Kim, and Hee-Joung Kim, "The effect of high-resolution parallel-hole collimator materials with a pixelated semiconductor SPECT system at equivalent sensitivities: Monte Carlo simulation studies." *Journal of the Korean Physical Society*, Vol. 64 (No. 7), pp. 1055-62, (2014).
- Alexandr I Kondrik, "Degradation Mechanisms of the Detector Properties of CdTe and CdZnTe Under the Influence of Gamma Irradiation." *East European Journal of Physics*, (No. 3), pp. 116-23, (2021).
- Xiaochun Lai, Liang Cai, Jia-Wei Tan, Elena Maria Zannoni, Boris Odintsov, and Ling-Jian Meng, "Design, Performance Evaluation, and Modeling of an Ultra-High Resolution Detector Dedicated for Simultaneous SPECT/MRI." *IEEE Transactions on Radiation and Plasma Medical Sciences*, (2021).
- Stefano Del Sordo, Leonardo Abbene, Ezio Caroli, Anna Maria Mancini, Andrea Zappettini, and Pietro Ubertini, "Progress in the development of CdTe and CdZnTe semiconductor radiation detectors for astrophysical and medical applications." *Sensors*, Vol. 9 (No. 5), pp. 3491-526, (2009).
- Abdul Basit, M Tariq Siddique, Sikander M Mirza, Shakeel Ur Rehman, and MY Hamza, "Study of CdTe detection efficiency for medical applications using Geant4-based stochastic simulations." *Journal of Radiological Protection*, Vol. 38 (No. 4), p. 1483, (2018).
- Samira Abbaspour, Babak Mahmoudian, and Jalil Pirayesh Islamian, "Cadmium telluride semiconductor detector for improved spatial and energy resolution radioisotopic imaging." *World journal of nuclear medicine*, Vol. 16 (No. 2), p. 101, (2017).
- Chan Rok Park, Seong-Hyeon Kang, and Youngjin Lee, "Similarity analysis of pixelated CdTe semiconductor gamma camera image using a quadrant bar phantom for nuclear medicine: Monte Carlo simulation study." *Nuclear Engineering and Technology*, Vol. 53 (No. 6), pp. 1947-54, (2021).
- Su Jin Park, Chang-Lae Lee, Hyo-Min Cho, and Hee-Joung Kim, "Ultra high resolution SPECT with CdTe for small animal imaging applications: Monte Carlo simulation study using voxelized phantom." in *Nuclear Science Symposium and Medical Imaging Conference (NSS/MIC), 2011 IEEE*, (2011): IEEE, pp. 3030-33.
- Katsutoshi Tsuchiya et al., "Basic performance and stability of a CdTe solid-state detector panel." *Annals of nuclear medicine*, Vol. 24 (No. 4), pp. 301-11, (2010).
- Tohru Shiga et al., "Dual isotope SPECT study with epilepsy patients using semiconductor SPECT system." *Clinical nuclear medicine*, Vol. 42 (No. 9), pp. 663-68, (2017).
- Elena Maria Zannoni et al., "Development of a multi-detector readout circuitry for ultrahigh energy resolution single-photon imaging applications." *Nuclear Instruments and Methods in Physics Research Section A: Accelerators, Spectrometers, Detectors and Associated Equipment*, Vol. 981p. 164531, (2020).
- Young-Jin Lee, Hyun-Ju Ryu, Hyo-Min Cho, Seung-Wan Lee, Yu-Na Choi, and Hee-Joung Kim, "Optimization of a high-resolution collimator for a CdTe detector: Monte Carlo simulation studies." *Journal of the Korean Physical Society*, Vol. 60 (No. 5), pp. 862-68, (2012).
- Yoshiyuki Hirano, Tsutomu Zeniya, and Hidehiro Iida, "Monte Carlo simulation of scintillation photons for the design of

- a high-resolution SPECT detector dedicated to human brain." *Annals of nuclear medicine*, Vol. 26 (No. 3), pp. 214-21, (2012).
- 20- Nikolas Sakellios *et al.*, "GATE simulations for small animal SPECT/PET using voxelized phantoms and rotating-head detectors." in *Nuclear Science Symposium Conference Record, 2006. IEEE*, (2006), Vol. 4: *IEEE*, pp. 2000-03.
- 21- Mahmoud Rasouli, Abbas Takavar, Mohammad Reza Ay, Sasan Saber, and George Loudos, "Effects of crystal pixel size and collimator geometry on the performance of a pixelated crystal γ -camera using Monte Carlo simulation." *Journal of nuclear medicine technology*, Vol. 38 (No. 4), pp. 199-204, (2010).
- 22- S-J Park *et al.*, "Evaluation of quantitative accuracy in CZT-based pre-clinical SPECT for various isotopes." *Journal of Instrumentation*, Vol. 10 (No. 05), p. T05004, (2015).
- 23- Chan Rok Park, Seong-Hyeon Kang, and Youngjin Lee, "Similarity analysis of pixelated CdTe semiconductor gamma camera image using a quadrant bar phantom for nuclear medicine: Monte Carlo simulation study." *Nuclear Engineering and Technology*, (2020).
- 24- Michael Ljungberg, "The SIMIND Monte Carlo program." *Monte Carlo calculations in nuclear medicine: Applications in diagnostic imaging*, Vol. 20126027(2012).
- 25- MT Bahreyni Toossi, J Pirayesh Islamian, M Momennezhad, M Ljungberg, and SH Naseri, "SIMIND Monte Carlo simulation of a single photon emission CT." *Journal of Medical Physics*, Vol. 35 (No. 1), p. 42, (2010).
- 26- Samira Abbaspour, Kaveh Tanha, Babak Mahmoudian, Majid Assadi, and Jalil Pirayesh Islamian, "A Monte Carlo study on the performance evaluation of a parallel hole collimator for a HiReSPECT: A dedicated small-animal SPECT." *Applied Radiation and Isotopes*, Vol. 139pp. 53-60, (2018).
- 27- John E Ejeh, Johan A van Staden, and Hanlie du Raan, "Validation of SIMIND Monte Carlo simulation software for modelling a siemens symbia T SPECT scintillation camera." in *World Congress on Medical Physics and Biomedical Engineering 2018*, (2019): *Springer*, pp. 573-76.
- 28- Jalil Pirayesh Islamian, Mohammad Taghi Bahreyni Toossi, Mehdi Momennezhad, Shahrokh Naseri, and Michael Ljungberg, "Simulation of a quality control Jaszczak Phantom with SIMIND monte carlo and adding the phantom as an accessory to the program." *Iranian Journal of Medical Physics*, Vol. 9 (No. 2), pp. 135-40, (2012).
- 29- Koichi Ogawa, Naoka Ohmura, Hirokazu Iida, Kayoko Nakamura, Tadaki Nakahara, and Atsushi Kubo, "Development of an ultra-high resolution SPECT system with a CdTe semiconductor detector." *Annals of nuclear medicine*, Vol. 23 (No. 8), pp. 763-70, (2009).
- 30- Andrew L Goertzen, Douglas W Jones, Jürgen Seidel, King Li, and Michael V Green, "First results from the high-resolution mouseSPECT annular scintillation camera." *IEEE transactions on medical imaging*, Vol. 24 (No. 7), pp. 863-67, (2005).
- 31- Y-J Lee *et al.*, "A Monte Carlo simulation study of the feasibility of a high resolution parallel-hole collimator with a CdTe pixelated semiconductor SPECT system." *Journal of Instrumentation*, Vol. 8 (No. 03), p. T03009, (2013).
- 32- Roberto Accorsi, Francesca Gasparini, and Richard C Lanza, "A coded aperture for high-resolution nuclear medicine planar imaging with a conventional Anger camera: experimental results." *IEEE transactions on nuclear science*, Vol. 48 (No. 6), pp. 2411-17, (2001).
- 33- Vahideh Moji *et al.*, "Performance evaluation of a newly developed high-resolution, dual-head animal SPECT system based on the NEMA NU1-2007 standard." *Journal of Applied Clinical Medical Physics*, Vol. 15 (No. 6), (2014).
- 34- Yujin Qi *et al.*, "Development and characterization of a high-resolution microSPECT system for small-animal imaging." in *Small-animal SPECT imaging: Springer*, (2005), pp. 259-66.
- 35- MT Bahreyni Toossi, J Pirayesh Islamian, M Momennezhad, M Ljungberg, and SH Naseri, "SIMIND Monte Carlo simulation of a single photon emission CT." *Journal of Medical Physics/Association of Medical Physicists of India*, Vol. 35 (No. 1), p. 42, (2010).
- 36- Jianhua Yan, Josh Schaefferkoetter, Maurizio Conti, and David Townsend, "A method to assess image quality for low-dose PET: analysis of SNR, CNR, bias and image noise." *Cancer Imaging*, Vol. 16 (No. 1), pp. 1-12, (2016).
- 37- Hyun-Ju Ryu, Young-Jin Lee, Seung-Wan Lee, Hyo-Min Cho, Yu-Na Choi, and Hee-Joung Kim, "Design of a high-resolution small-animal SPECT-CT system sharing a CdTe semiconductor detector." *Journal of the Korean Physical Society*, Vol. 61 (No. 1), pp. 130-34, (2012).
- 38- L Verger *et al.*, "Characterization of CdTe and CdZnTe detectors for gamma-ray imaging applications." *Nuclear Instruments and Methods in Physics Research Section A: Accelerators, Spectrometers, Detectors and Associated Equipment*, Vol. 458 (No. 1), pp. 297-309, (2001).
- 39- Paolo Russo, Giovanni Mettivier, R Pani, R Pellegrini, MN Cinti, and P Bennati, "Imaging performance comparison between a LaBr₃:Ce scintillator based and a CdTe semiconductor based photon counting compact gamma camera." *Medical physics*, Vol. 36 (No. 4), pp. 1298-317, (2009).
- 40- W-S Choong, WW Moses, CS Tindall, and PN Luke, "Design for a high-resolution small-animal SPECT system using pixelated Si (Li) detectors for in vivo ¹²⁵I imaging." *IEEE transactions on nuclear science*, Vol. 52 (No. 1), pp. 174-80, (2005).
- 41- Hirokazu Iida and Koichi Ogawa, "Comparison of a pixelated semiconductor detector and a non-pixelated scintillation detector in pinhole SPECT system for small animal study." *Annals of nuclear medicine*, Vol. 25 (No. 2), pp. 143-50, (2011).
- 42- Michał Błaszczyk, Zbigniew Adamczewski, and Anna Płachcińska, "Capabilities of Modern Semiconductor Gamma Cameras in Radionuclide Diagnosis of Coronary Artery Disease." *Diagnostics*, Vol. 11 (No. 11), p. 2130, (2021).
- 43- Atsuro Suzuki *et al.*, "High-sensitivity brain SPECT system using cadmium telluride (CdTe) semiconductor detector and 4-pixel matched collimator." *Physics in medicine and biology*, Vol. 58 (No. 21), p. 7715, (2013).

- 44- Yasuyuki Takahashi, Masao Miyagawa, Yoshiko Nishiyama, Naoto Kawaguchi, Hayato Ishimura, and Teruhito Mochizuki, "Dual radioisotopes simultaneous SPECT of ^{99m}Tc -tetrofosmin and ^{123}I -BMIPP using a semiconductor detector." *Asia Oceania Journal of Nuclear Medicine and Biology*, Vol. 3 (No. 1), pp. 43-49, (2015).